



## Helium-cluster decay widths of molecular states in beryllium and carbon isotopes

J.C. Pei <sup>a</sup>, F.R. Xu <sup>a,b,c,\*</sup>

<sup>a</sup> School of Physics and MOE Laboratory of Heavy Ion Physics, Peking University, Beijing 100871, China

<sup>b</sup> Institute of Theoretical Physics, Chinese Academy of Sciences, Beijing 100080, China

<sup>c</sup> Center of Theoretical Nuclear Physics, National Laboratory of Heavy Ion Collisions, Lanzhou 730000, China

Received 29 December 2006; received in revised form 30 March 2007; accepted 15 May 2007

Available online 23 May 2007

Editor: J.-P. Blaizot

### Abstract

<sup>4</sup>He (i.e.,  $\alpha$  particle) and <sup>6</sup>He emissions from possible molecular states in beryllium and carbon isotopes have been investigated using a mean-field-type cluster potential. Calculations can reasonably describe the  $\alpha$ -decay widths of studied states in beryllium and carbon isotopes, and also <sup>20</sup>Ne, compared with experiments. For the nucleus <sup>10</sup>Be, we discussed  $\alpha$ -decay widths with different shapes or different decay modes, in order to understand the very different decay widths of two excited states. The widths of <sup>6</sup>He decays from <sup>12</sup>Be and  $\alpha$  decays from <sup>13,14</sup>C are predicted, which could be useful for future experiments.

© 2007 Elsevier B.V. Open access under [CC BY license](http://creativecommons.org/licenses/by/3.0/).

PACS: 21.60.Gx; 21.10.Tg; 23.90.+w; 27.20.+n

Keywords: Mean-field potential; Cluster structure; Decay width; Beryllium; Carbon

The experimental search for molecular-type structures in light nuclei is of increasing interest. The Ikeda diagram as a guideline reveals that cluster structures in light nuclei are expected to appear in the vicinities of decay thresholds [1]. Evidences for dimers in beryllium isotopes and polymers in carbon isotopes have been summarized by von Oertzen [2]. It is convincing that the large moments of inertia in rotational cluster bands correspond to molecular-like structures. For cluster states above thresholds, one can further understand their properties through the measurements and calculations of cluster decay widths. The model calculations of decay widths usually involve cluster potentials that can be related to the angular momenta and possible deformations of nuclear states, providing useful structure information about cluster states.

In the nucleus <sup>8</sup>Be, a rotational cluster band and its decay property have been well established based on the  $\alpha$ - $\alpha$  struc-

ture [3]. In heavier beryllium isotopes, two  $\alpha$ -particles and additional valence neutrons can give rise to covalent molecular binding. Recent experiments have observed the  $\alpha + ^6\text{He}$  decay from excited states in <sup>10</sup>Be [4,5] and the <sup>6</sup>He + <sup>6</sup>He decay in <sup>12</sup>Be [6,7], suggesting molecular structures in the nuclei [4–7]. Different molecular states in <sup>10</sup>Be and <sup>12</sup>Be have been discussed by antisymmetrized molecular dynamics (AMD) calculations [8,9]. It is intriguing that carbon isotopes with three  $\alpha$ -clusters can have two different configurations: triangular and chain. For <sup>13</sup>C and <sup>14</sup>C, cluster bands based on the  $\alpha + ^9\text{Be}$  and  $\alpha + ^{10}\text{Be}$  structures have been proposed [2,10,11], respectively, with increasing experimental interests in the measurements of their  $\alpha$  decays [12,13].

Many theoretical works (e.g., [14–20]) have shown the success of the WKB approach in the calculations of cluster decay lifetimes for the various mass regions of nuclei. With the combining use of the Bohr–Sommerfeld quantization, Buck et al. have achieved the calculations of spectra of rotational cluster bands using macroscopic cluster potentials [21]. Recently, we suggested a microscopic cluster potential based on the mean-field model [22]. The mean-field-type cluster potential has been

\* Corresponding author at: School of Physics and MOE Laboratory of Heavy Ion Physics, Peking University, Beijing 100871, China.  
E-mail address: [frxu@pku.edu.cn](mailto:frxu@pku.edu.cn) (F.R. Xu).

successfully applied to the calculations of the cluster-decay lifetimes of ground states (g.s.) in even–even heavy nuclei, without raising any adjustable parameter [22]. In the present work, we extend our calculations by including the deformations and angular momenta of cluster states. We focus on the cluster decays of excited states in light nuclei, particularly in beryllium and carbon isotopes that are attracting great interest in experiments.

The cluster potential in quantum tunnelling calculations can be written as (e.g., [14])

$$V(r) = V_N(r) + V_C(r) + \frac{\hbar^2}{2\mu r^2} \left( L + \frac{1}{2} \right)^2, \quad (1)$$

that contains the nuclear potential  $V_N(r)$ , the Coulomb potential  $V_C(r)$  and the Langer modified centrifugal potential with  $L$  and  $\mu$  for the angular momentum of the cluster and the reduced mass of the cluster-core system, respectively [14]. In our previous work [22], the nuclear potential between the cluster and the remaining core has been suggested as follows,

$$V_N(r) = \lambda [N_c v_n(r) + Z_c v_p(r)], \quad (2)$$

where  $\lambda$  is the folding factor;  $N_c$  and  $Z_c$  are the neutron and proton numbers of the cluster, respectively;  $v_n(r)$  and  $v_p(r)$  are the single-neutron and -proton potentials (excluding the Coulomb potential), respectively, generated by the core. The single-particle potentials are obtained using the self-consistent Skyrme–Hartree–Fock (SHF) model with the SLy4 force [23]. In the SHF model, single-particle potentials are calculated by using neutron and proton densities that are obtained from the nucleon wave functions of the SHF calculation [24]. Therefore, the mean-field-type cluster potential, due to the interdependence of neutron and proton densities, contains a dependence on nucleon numbers, i.e., an isospin dependence, in a self-consistent manner. The Coulomb potential  $V_C(r)$  is well defined physically and should not be folded. We have approximated the Coulomb potential by  $V_C(r) = Z_c v_c(r)$ , where  $v_c(r)$  is the single-proton Coulomb potential calculated with the density of the protons in the core.

The folding factor  $\lambda$  is determined using the Bohr–Sommerfeld quantization condition [14],

$$\int_{r_1}^{r_2} \sqrt{\frac{2\mu}{\hbar^2} |Q_L^* - V(r)|} = (2n + 1) \frac{\pi}{2} = (G - L + 1) \frac{\pi}{2}, \quad (3)$$

where  $r_1$ ,  $r_2$  (and  $r_3$  later) are classical turning points obtained by  $V(r) = Q_L^*$  (the decay energy). The global quantum number  $G = 2n + L$  ( $n$  is the node number in the radial wave function of the cluster tunnelling motion) is determined by the Wildermuth rule [25], depending on the configurations of cluster nucleons. The cluster decay energy from an excited state is given by

$$Q_L^* = Q_0 + E_J^*, \quad (4)$$

where  $Q_0$  is the decay energy from the ground state, and  $E_J^*$  is the excitation energy of a given state with the spin of  $J$ . The decay process can occur only if the state has a positive  $Q_L^*$  value (i.e., above threshold). Since the decay calculation is very sensitive to the  $Q_L^*$  value, experimental  $Q_0$  and  $E_J^*$  values have been adopted in calculations.

The partial cluster decay width is calculated by (see, e.g., [14])

$$\Gamma = P \frac{(\hbar^2/4\mu) \exp[-2 \int_{r_2}^{r_3} dr k(r)]}{\int_{r_1}^{r_2} dr/2k(r)}, \quad (5)$$

where  $k(r) = \sqrt{\frac{2\mu}{\hbar^2} |Q_L^* - V(r)|}$  is the wave number, and  $P$  is the preformation factor of the cluster being formed in the mother nucleus. For even–even nuclei, it has been shown that the extreme  $P = 1$  assumption under the use of the Bohr–Sommerfeld condition can well reproduce the experimental half-lives of various cluster decays [14,22]. The decay half-life can be obtained by  $T_{1/2} = \hbar \ln 2 / \Gamma$ .

Usually, nuclei can be treated as spherical systems in the tunnelling calculations of cluster decays [14–22]. The formulae above give a simple one-dimensional calculation of the cluster decay. For nuclei with very large deformations, however, the deformation modification may be needed. As an approximation for axial deformed nuclei, the decay width can be modified by averaging widths in the various directions of the space as follows [26]

$$\Gamma = \int_0^{\pi/2} \Gamma(\theta) \sin \theta d\theta, \quad (6)$$

where  $\Gamma(\theta)$  is the decay width of the cluster emitted in the direction of a  $\theta$ -angle away from the symmetry axis, calculated using the one-dimensional formulae above. In the deformation case, deformed potentials are needed, that can be obtained by the shape-constrained SHF calculation [27]. For simplicity, the folding factor  $\lambda$  determined at the spherical shape has been used.

In our previous work [22], the cluster decays of heavy nuclei have been investigated. However, recent experiments suggest that the decays of light nuclei are more challenging due to their interesting cluster structures, particularly for exotic states. As the examples of the cluster decays of light nuclei, we have firstly calculated the  $^8\text{Be}$  and  $^{20}\text{Ne}$  nuclei in which  $\alpha$ -cluster structures have been well known [25], with rotational cluster bands (spectra) observed [28]. Their cluster properties have been well described by the semiclassical cluster model [3,21]. In calculations, one needs to determine the global quantum number  $G$ . For  $^8\text{Be}$ , we take  $G = 4$  for the g.s. band, according to the Wildermuth rule [25]. In  $^{20}\text{Ne}$ ,  $G = 8$  has been taken for the  $K^\pi = 0^+$  g.s. band and  $G = 9$  for the  $K^\pi = 0^-$  band, as discussed in Refs. [21,25]. Calculated results at the spherical shape are given in Table 1. It can be seen that the present calculations agree well with experimental widths [28] within a factor of 3.  $^{20}\text{Ne}$  is an interesting nucleus that can have very different structures for different states. While the  $K^\pi = 0^-$  band with the sequence of  $J^\pi = 1^-, 3^-, \dots, 9^-$  has an almost pure  $\alpha + ^{16}\text{O}$  cluster structure, the  $0^+$  g.s. band has a considerable mixture of the cluster configuration and the deformed mean-field structure [29]. For the  $0^-$  band, both experiments and our calculations give large  $\alpha$ -decay widths that are comparable with the Wigner limit [29], indicating the significant  $\alpha + ^{16}\text{O}$  cluster structure.

Table 1  
Calculated  $\alpha$ -decay widths of excited states in  $^8\text{Be}$  and  $^{20}\text{Ne}$ , compared with experimental data [28]

$J^\pi$	$E_j^*$ [28] (MeV)	$(G, L)$	$\Gamma_\alpha(\text{cal.})$ (keV)	$\Gamma_\alpha(\text{expt.})$ (keV)
$^8\text{Be} (Q_0 = 91.8 \text{ keV})$				
$0^+$	0.00	(4, 0)	7.8 eV	$6.8 \pm 1.7 \text{ eV}$
$2^+$	3.04	(4, 2)	$1.6 \times 10^3$	$1.5 \times 10^3$
$4^+$	11.40	(4, 4)	$2.3 \times 10^3$	$\approx 3.5 \times 10^3$
$^{20}\text{Ne} (Q_0 = -4.729 \text{ MeV})$				
$6^+$	8.78	(8, 6)	0.17	$0.11 \pm 0.02$
$8^+$	11.95	(8, 8)	90 eV	$35 \pm 10 \text{ eV}$
$1^-$	5.79	(9, 1)	18 eV	$28 \pm 3 \text{ eV}$
$3^-$	7.16	(9, 3)	4.7	$8.2 \pm 0.3$
$5^-$	10.26	(9, 5)	54	$145 \pm 40$
$7^-$	15.37	(9, 7)	120	$110 \pm 10$
$9^-$	22.87	(9, 9)	116	$225 \pm 40$

Table 2  
Calculated and experimental widths of observed  $\alpha$  decays from the  $2^+$  and  $4^+$  states of the  $0_2^+$  cluster band in  $^{10}\text{Be}$  ( $Q_0 = -7.413 \text{ MeV}$ ). Calculations have been performed at spherical ( $\Gamma_\alpha(\text{sph.})$ ) and deformed ( $\Gamma_\alpha(\text{def.})$ ) shapes.  $\Gamma_\alpha(z\text{-axis})$  is the calculation assuming the  $\alpha$  particle emitting along the symmetry axis only

$J^\pi$	$E_j^*$ (MeV)	$\Gamma_\alpha(\text{sph.})$	$\Gamma_\alpha(\text{def.})$	$\Gamma_\alpha(z\text{-axis})$	$\Gamma_\alpha(\text{expt.})$
$2^+$	7.54 [4]	0.51 eV	0.85 eV	4.1 eV	$22 \pm 7 \text{ eV}$ [4]
$4^+$	10.15 [5]	35 keV	97 keV	584 keV	130 keV [5]

In light nuclei, more interesting are exotic molecular states with additional covalent neutrons moving between clusters [4–7]. Excited molecular-like states with an  $\alpha:2n:\alpha$  cluster structure in  $^{10}\text{Be}$  [4,5] and an  $\alpha:4n:\alpha$  structure in  $^{12}\text{Be}$  [6,7] have been suggested experimentally. In  $^{10}\text{Be}$ , a rotational cluster band with the members of  $0_2^+$  (6.18 MeV),  $2^+$  (7.54 MeV) and  $4^+$  (10.15 MeV) has been established in experiments [5,30]. The  $2\alpha$  structure leads to the elongated shapes of the nuclei. Predicted by the molecular orbital model [31], the distance between two  $\alpha$ -particles in the  $0_2^+$  state of  $^{10}\text{Be}$  is about 4 fm, which gives an axis ratio of 2.5:1, corresponding to a prolate deformation of  $\beta_2 \approx 1.1$ . At such a large prolate deformation, the states of the  $0_2^+$  cluster band have two valence neutrons occupying the  $sd_{1/2}$  orbits [31], which leads to a global number of  $G = 6$  in our WKB calculations. Table 2 lists calculated  $\alpha$ -decay widths for states belonging to the  $K^\pi = 0_2^+$  cluster band in  $^{10}\text{Be}$ . The bandhead (i.e., the  $0_2^+$  state) has a negative  $Q_L^*$  value (i.e., below threshold) and hence no  $\alpha$  decay happens for the state.

From Table 2, it can be seen that calculations at the spherical shape give much smaller  $\alpha$ -decay widths than experimental data. The observed width of the  $4^+$  state can be reasonably reproduced in the calculation with the deformation of  $\beta_2 = 1.1$ . However, the decay width of the  $2^+$  state is still much underestimated. The  $2^+$  state is above the decay threshold by only 127 keV. For a state near threshold, the decay width is particularly sensitive to the decay energy. We find that an increase of only 50 keV in the decay energy can reproduce the experimental decay width of the  $2^+$  state. Considering the  $\alpha:2n:\alpha$

Table 3  
Calculated  $^6\text{He}$ -decay widths of states belonging to the  $K^\pi = 0_3^+$  band in  $^{12}\text{Be}$  ( $Q_0 = -10.11 \text{ MeV}$ ). Experimental excitation energies  $E_j^*$  are taken from [6]. AMD predictions [9] are also given for comparison

$J^\pi$	$E_j^*$ (MeV)	$\Gamma_{^6\text{He}}(\text{sph.})$ (keV)	$\Gamma_{^6\text{He}}(\text{def.})$ (keV)	$\Gamma_{^6\text{He}}$ [9] (keV)
$0_3^+$	10.9	410	620	700
$2^+$	11.3	285	300	1
$4^+$	13.2	190	280	7
$6^+$	16.1	34	110	16
$8^+$	20.9	3.7	18	

molecular structure in the  $0_2^+$  band [5], we suggest another possibility in which the  $\alpha$  particle emits along the  $z$ -axis only (i.e., the long axis in the prolate shape). Such a calculation gives a significantly improved decay width for the  $2^+$  state (see Table 2). However, the width of the  $4^+$  state is overestimated. In Refs. [31,32], it was pointed out that the states of the  $0_2^+$  band could contain the mixture of the  $^5\text{He} + ^5\text{He}$  configuration. The mixture would be more remarkable for the  $4^+$  state because it is almost on the  $^5\text{He} + ^5\text{He}$  decay threshold. The  $^5\text{He} + ^5\text{He}$  mixture results in a reduction of the  $\alpha$ -decay width.

In the neutron-rich nucleus  $^{12}\text{Be}$ , resonance states have been observed, decaying to  $\alpha + ^8\text{He}$  and  $^6\text{He} + ^6\text{He}$  channels, which suggests molecular cluster states [6,7]. AMD calculations showed that the resonance can happen in molecular states built on the  $0_3^+$  configuration [9]. Considering that the highest excited state in the  $0_3^+$  band is the  $8^+$  level [6,7], we take  $G = 8$  in the  $^6\text{He} + ^6\text{He}$  decay calculation. The spherical and deformed calculations have been performed (given in Table 3) with comparison with AMD predictions [9]. Given by AMD calculations [9],  $\beta_2 = 0.7$  has been taken in the deformed calculations. As predicted in [9], the  $^6\text{He}$ -decay width of the  $0_3^+$  state is very large, partly due to the lack of the centrifugal barrier. Listed in the last column of Table 3, AMD calculations gave a dramatic decrease in widths from the  $0_3^+$  state to the  $J \geq 2$  states, which means remarkable reductions in the preformation factors of the  $^6\text{He}$  cluster in the  $J \geq 2$  states [9]. To check theoretical predictions, the experimental measurements of the  $^6\text{He}$ -decay widths are required. The measurement is also very helpful for the better understanding of the molecular structure [6].

Compared with beryllium isotopes, carbon nuclei have more complicated geometric structures with three  $\alpha$ -clusters. As suggested in Refs. [10,11], there are possible prolate (chain) and oblate (triangular) cluster structures in carbon isotopes. The chain and triangular structures can lead to different decay widths. Fig. 1 shows a schematic picture for two possible  $\alpha$ -decay modes in  $^{12}\text{C}$ . An  $\alpha$ - $\alpha$  core has been assumed, which gives a deformed cluster potential with an axis ratio of 2:1 (corresponding to  $\beta_2 = 0.8$ ). In  $^{12}\text{C}$ , it has been well known that there are an oblate g.s. band with  $0^+$ ,  $2^+$ ,  $4^+$  members and a negative-parity oblate band built on the  $3^-$  (9.641 MeV) state (though the  $4^-$  and  $5^-$  levels have not been found experimentally) [13]. For carbon isotopes, we have calculated their  $\alpha$ -decay widths with assuming the  $\alpha$  particle emitting in the direction of  $\theta = \pi/2$  (oblate) or  $\theta = 0$  (prolate), as shown in Fig. 1. Experimentally, the partial widths of the  $\alpha$  decays have

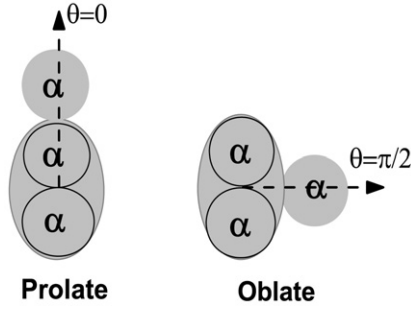


Fig. 1. Schematic picture for two modes of  $\alpha$  decays in carbon isotopes, corresponding to the prolate (chain) and oblate (triangular) structures.

Table 4

Calculated  $\alpha$ -decay widths of excited states in carbon isotopes. Experimental total decay widths ( $\Gamma$ ) and excitation energies ( $E_j^*$ ) are taken from [28] for  $^{12,13}\text{C}$  and from [11] for  $^{14}\text{C}$

$J^\pi$	$E_j^*$ (MeV)	( $G, L$ )	$\Gamma_\alpha$ (cal.) (keV)	$\Gamma$ (expt.) (keV)
$^{12}\text{C}$ ( $Q_0 = -7.366$ MeV)				
$3_1^-$	9.641	(5, 3)	17	$34 \pm 5$
$4_1^+$	14.08	(4, 4)	158	$258 \pm 15$
$0_2^+$	7.654	(6, 0)	5.9 eV	$8.5 \pm 1.0$ eV
$^{13}\text{C}$ ( $Q_0 = -10.647$ MeV)				
$K^\pi = 3/2^-$				
$5/2^-$	10.82	(6, 2)	0.2 eV	$24 \pm 3$
$7/2^-$	12.44	(6, 2)	84	$140 \pm 30$
$9/2^-$	14.13	(6, 4)	32	$\approx 150$
$11/2^-$	16.08	(6, 4)	316	$150 \pm 15$
$K^\pi = 3/2^+$				
$3/2^+$	11.08	(7, 1)	41 eV	$\leq 4$
$5/2^+$	11.95	(7, 1)	100	$500 \pm 80$
$7/2^+$	13.41	(7, 3)	112	$35 \pm 3$
$9/2^+$	15.28	(7, 3)	888	
$11/2^+$	16.95	(7, 5)	125	330
$^{14}\text{C}$ ( $Q_0 = -12.011$ MeV)				
$5^-$	14.87	(7, 5)	0.4	35
$6^+$	16.43	(6, 6)	0.12	35
$3^-$	12.58	(7, 3)	22 eV	95
$5^-$	15.18	(7, 5)	31	50
$7^-$	18.03	(7, 7)	14	70
$6^+$	14.67	(6, 6)	0.21	40

not been available. However, the states have almost pure  $\alpha$ -decay channels [28,33], and hence we use the total decay width  $\Gamma$  for comparison. Shown in Table 4, oblate calculations give reasonable widths compared with experimental total widths. Prolate calculations give 243 keV and 2.2 MeV for the  $\alpha$ -decay widths of the  $3_1^-$  and  $4_1^+$  states, respectively, that are one order of magnitude larger than the oblate calculations. Therefore, our calculations support triangular cluster structures for the  $3_1^-$  and  $4_1^+$  states. The  $0_1^+$  and  $2_1^+$  states of the g.s. band are below the threshold without  $\alpha$  decay happening.

In  $^{12}\text{C}$ , there is a famous excited  $0^+$  state (Hoyle state) that was predicted by Hoyle in 1950s to understand the observed abundance of  $^{12}\text{C}$  in the universe [34]. The excitation energy of the  $0_2^+$  state should be near the threshold of the  $\alpha + ^8\text{Be}$  fusion, in order to obtain the accelerated synthesis of the  $^{12}\text{C}$

element in the beginning of the universe [34]. The Hoyle state was confirmed soon experimentally at the excitation energy of 7.654 MeV [35]. The  $\alpha$  decay of the  $0_2^+$  state has been studied with the triple cluster model [33]. This state has a decay energy of 288 keV to  $\alpha + ^8\text{Be}$ (g.s.) and an energy of 380 keV to the  $3\alpha$  channel. For the decay to  $\alpha + ^8\text{Be}$ , the present calculation with a chain structure ( $\beta_2 = 0.8$ ) gives an  $\alpha$  width of 5.9 eV that agrees with the observed value of 8.5 eV. The calculation assuming a triangular configuration leads to a smaller width of 1.6 eV. For the decay to the  $3\alpha$  channel with a triangular structure, our model estimates a width of 36 eV that is close to the predictions of the AMD [36] and triple cluster models [33]. However, the contribution of the direct  $3\alpha$  decay to the total width is less than 4%, determined in the experiment [37]. Hence, the chain cluster decay to  $\alpha + ^8\text{Be}$  would dominate the decay of the  $0_2^+$  state in  $^{12}\text{C}$ .

In the neutron-odd isotope  $^{13}\text{C}$ , the  $K^\pi = 3/2^\pm$  bands built on the  $\alpha + ^9\text{Be}$  ( $3/2^-,$  g.s.) configuration have been suggested experimentally [10]. The parity doublet bands are related to reflection-asymmetric chain configurations, corresponding to a large prolate deformation [10]. We assume that the core (i.e.,  $^9\text{Be}$ ) has a similar deformation to that of the ground state of  $^{10}\text{Be}$  with  $\beta_2 \approx 0.6$  estimated experimentally [38]. In  $\alpha$ -width calculations, we take  $G = 6$  and  $7$  for the  $K^\pi = 3/2^-$  and  $3/2^+$  bands, respectively, considering the different parities of these two bands. The angular momentum  $L$  that the  $\alpha$  particle carries is obtained by the angular momentum selection among the mother, daughter and  $\alpha$  particle. Furthermore, for the odd nucleus  $^{13}\text{C}$ , we take a preformation factor of  $P = 0.6$  that was adopted in the systematic  $\alpha$ -decay calculations of odd nuclei in Ref. [14]. The calculated  $\alpha$  widths of the  $K^\pi = 3/2^\pm$  band members are listed in Table 4. Experimental partial  $\alpha$ -widths have not been available, but we give the experimental total decay widths  $\Gamma$  [10,28] for comparison.

Calculated  $\alpha$  widths in  $^{13}\text{C}$  are in general smaller than experimental total widths, as expected. However, calculated values for  $11/2^-$  (16.08 MeV) and  $7/2^+$  (13.41 MeV) states [10] are larger than experimental total widths. In Ref. [28], the 16.08 and 13.41 MeV states were assigned with other possible configurations of  $7/2^+$  and  $9/2^-$ , respectively. The recent experiment [13] suggests that the 16.08 MeV state has a positive parity and the 13.41 MeV state has an oblate structure. Calculations can be changed significantly due to the different assignments of configurations.

The heavier carbon isotope,  $^{14}\text{C}$ , is attracting great interest in experiments, with triangular and chain cluster bands suggested [11]. Also in Table 4, we give our predictions for the  $\alpha$  widths of  $^{14}\text{C}$  decaying to the g.s. of  $^{10}\text{Be}$ . In the table, the first two states (i.e., 14.87 and 16.43 MeV states) have triangular structures and other states have chain shapes [11]. The calculated width of the  $3^-$  (12.58 MeV) state is remarkably smaller than the experimental total width. This would indicate that the neutron emission dominates the decay of the state that is near the  $\alpha$ -decay threshold. The  $\alpha$ -decay channel from the  $6^+$  (16.43 MeV) state to the excited  $2^+$  (3.37 MeV) state of  $^{10}\text{Be}$  has been observed though it is very weak [39]. The decay width in the present calculation is estimated to be 5 eV, giving

Table 5  
Calculated  $\alpha$  widths of highly excited states in  $^{14}\text{C}$  decaying to the g.s. and the first  $2^+$  state of  $^{10}\text{Be}$

$J^\pi$	18.5 MeV		19.8 MeV	
	$^{10}\text{Be}(\text{g.s.})$	$^{10}\text{Be}(2^+)$	$^{10}\text{Be}(\text{g.s.})$	$^{10}\text{Be}(2^+)$
$4^+$	1.2 MeV	0.8 MeV	2.7 MeV	
$6^+$	11 keV	30 keV	41 keV	230 keV
$5^-$	0.28 MeV	0.39 MeV	0.7 MeV	1.2 MeV
$7^-$	0.8 keV	2.3 keV	3.5 keV	25 keV

a small branching ratio of 4% relative to the channel to the g.s. of  $^{10}\text{Be}$ .

In  $^{14}\text{C}$ , it is interesting that higher excited states at the excitation energies of 18.5 and 19.8 MeV have strong decay channels to both the g.s. and the first  $2^+$  state of  $^{10}\text{Be}$  [12,39]. No experimental assignments of spins and parities have been available for these two states. We estimated their  $\alpha$ -decay widths with assuming  $J^\pi = 4^+, 6^+$  ( $G = 6$ ) and  $J^\pi = 5^-, 7^-$  ( $G = 7$ ). Calculations are performed with the simple spherical shape. As shown in Table 5, the calculated  $\alpha$  widths are sensitive to the assignments of angular momenta. With the spins of  $J = 4$  and  $5$ , broad widths are obtained for both channels, as observed in experiments [12,39].

In summary, we have investigated helium-cluster decay widths in beryllium and carbon isotopes using a mean-field-type cluster potential in the WKB approach. The cluster potential is obtained from the self-consistent Skyrme–Hartree–Fock calculation, containing the isospin dependence automatically. The calculations give, in general, the good descriptions of cluster decay properties in the isotopes. With deformed cluster potentials, we have discussed the helium-decay widths of excited  $2\alpha$  molecular states in  $^{10,12}\text{Be}$  and  $3\alpha$  triangular and chain states in  $^{12,13,14}\text{C}$ . However, deformation parameters that have been used in the calculations are not observable, and their values are usually model-dependent. Systematic comparisons with existing experimental data have been made, providing some useful information about the structures and decay modes of the cluster states. In the present work, we have focused mainly on cluster decays from the excited states of mothers to the ground states of daughters. For highly excited resonance states, however, decays to the excited states of daughters would be possible.

### Acknowledgements

We are grateful to Dr. M. Milin for valuable comments and Dr. P.D. Stevenson for providing the Skyrme–Hartree–Fock code. This work has been supported by the Natural Science Foundation of China under Grant Nos. 10525520 and 10475002, and the Key Grant Project (Grant No. 305001) of

Education Ministry of China. We also thank the PKU Computer Center where numerical calculations have been done.

### References

- [1] K. Ikeda, N. Takigawa, H. Horiuchi, Prog. Theor. Phys. (Japan) (Suppl. Extra Number) (1968) 464.
- [2] W. von Oertzen, Z. Phys. A 354 (1996) 37; W. von Oertzen, Z. Phys. A 357 (1997) 355; W. von Oertzen, Nucl. Phys. A 738 (2004) 264.
- [3] B. Buck, H. Friedrich, C. Wheatley, Nucl. Phys. A 275 (1977) 246.
- [4] J.A. Liendo, N. Curtis, D.D. Caussyn, N.R. Fletcher, T. Kurtukian-Nieto, Phys. Rev. C 65 (2002) 034317.
- [5] M. Freer, et al., Phys. Rev. Lett. 96 (2006) 42501.
- [6] M. Freer, et al., Phys. Rev. Lett. 82 (1999) 1383.
- [7] A. Saito, et al., Nucl. Phys. A 738 (2004) 337.
- [8] Y. Kanada-En'yo, H. Horiuchi, A. Doté, Phys. Rev. C 60 (1999) 064304.
- [9] Y. Kanada-En'yo, H. Horiuchi, Phys. Rev. C 68 (2003) 014319.
- [10] M. Milin, W. von Oertzen, Eur. Phys. J. A 14 (2002) 295.
- [11] W. von Oertzen, et al., Eur. Phys. J. A 21 (2004) 193.
- [12] N. Soić, et al., Phys. Rev. C 68 (2003) 014321.
- [13] D.L. Price, et al., Nucl. Phys. A 765 (2006) 263.
- [14] B. Buck, A.C. Merchant, S.M. Perez, Phys. Rev. Lett. 65 (1990) 2975; B. Buck, A.C. Merchant, S.M. Perez, At. Data Nucl. Data Tables 54 (1993) 53.
- [15] D.S. Delion, A. Insolia, R.J. Liotta, Phys. Rev. C 46 (1992) 1346.
- [16] C. Xu, Z.Z. Ren, Phys. Rev. C 69 (2004) 024614; C. Xu, Z.Z. Ren, Nucl. Phys. A 60 (2005) 303; Z.Z. Ren, C. Xu, Z.J. Wang, Phys. Rev. C 70 (2004) 034304.
- [17] P. Mohr, Phys. Rev. C 61 (2000) 045802; P. Mohr, Phys. Rev. C 73 (2006) 031301(R).
- [18] S. Ohkubo, Phys. Rev. Lett. 74 (1995) 2176.
- [19] P.R. Chowdhury, C. Samanta, D.N. Basu, Phys. Rev. C 73 (2006) 014612.
- [20] Z.A. Dupré, T.J. Bürvenich, Nucl. Phys. A 767 (2006) 81.
- [21] B. Buck, A.C. Merchant, S.M. Perez, Phys. Rev. C 51 (1995) 559.
- [22] F.R. Xu, J.C. Pei, Phys. Lett. B 642 (2006) 322.
- [23] E. Chabanat, P. Bonche, P. Hasensel, J. Meyer, R. Schaeffer, Nucl. Phys. A 635 (1998) 231.
- [24] D. Vautherin, Phys. Rev. C 7 (1973) 296.
- [25] K. Wildermuth, Y.C. Tang, A Unified Theory of the Nucleus, Academic Press, New York, 1977.
- [26] V.Yu. Denisov, H. Ikezoe, Phys. Rev. C 72 (2005) 064613.
- [27] J.C. Pei, F.R. Xu, P.D. Stevenson, Nucl. Phys. A 765 (2006) 29.
- [28] R.B. Firestone, V.S. Shirley (Eds.), Table of Isotopes, eighth ed., Wiley, New York, 1996.
- [29] M. Kimura, Phys. Rev. C 69 (2004) 044319.
- [30] M. Milin, et al., Nucl. Phys. A 753 (2005) 263.
- [31] N. Itagaki, S. Okabe, Phys. Rev. C 61 (2000) 044306.
- [32] M. Ito, K. Kato, K. Ikeda, Phys. Lett. B 588 (2004) 43.
- [33] D.V. Fedorov, A.S. Jensen, H.O.U. Fynbo, Nucl. Phys. A 718 (2003) 685; D.V. Fedorov, A.S. Jensen, Phys. Lett. B 389 (1996) 631.
- [34] F. Hoyle, Astrophys. J. Suppl. Ser. 1 (1954) 121.
- [35] C.W. Cook, et al., Phys. Rev. 107 (1957) 508.
- [36] Y. Kanada-En'yo, nucl-th/0605047.
- [37] M. Freer, et al., Phys. Rev. C 49 (1994) R1751.
- [38] H. Iwasaki, et al., Phys. Lett. B 481 (2000) 7.
- [39] M. Milin, et al., Nucl. Phys. A 730 (2004) 285.